Optimal Shape of DC Electromagnet

Alin-Iulian Dolan
University of Craiova, Faculty of Electrical Engineering, Craiova, Romania, adolan@elth.ucv.ro

***Abstract* – In this paper is proposed an optimal geometrical shape for a DC electromagnet by combining the design of experiments (DOE) and 2-D FEM. The optimization problem takes into account four geometrical parameters (the coil shape ratio, the support thickness ratio, the support height ratio and the support top ratio) and consists in maximization of the acting force related to the largest air-gap, preserving the global dimensions of the device (the external radius, the height of carcass, the height of plunger with support) and the cross-section of the winding. Before optimization, the technique of screening was applied to verify the influence of the four geometrical parameters on the acting force. The experiments were performed by numerical tool FEMM in relation to the LUA language. The acting force was computed by Maxwel Stress Tensor principle. Best influence was observed for all the four parameters, especially for the support top ratio, with 99% confidence. The method by zooms without computation of models was applied to increase with 21.20% the acting force related to the air-gap of 41 mm. The cost of this improvement is the reduction of electromagnetic force for lower air-gaps which can be compensated by eliminating the economy resistor in this range.**

Cuvinte cheie: *optimizare, programarea experimentelor, metoda elementelor finite 2-D.*

Keywords: *optimization, DOE, 2-D FEM.*

I. Introduction

The numerical experiments successfully replace the real ones especially in solving optimization problems in electromagnetism, combining experimental design (DOE) with finite element method (FEM) [1] – [4].

The response surface methodology (RSM), as one of the branches of DOE, is combined with FEM in [5] to make a screening of significant parameters of an electrical motor in order to optimize its performances. The same techniques were applied in [6] to improve an electromagnet in magnetic levitation system based on many design variables.

The maximization of the force developed by an electromagnetic actuator was often an appropriate case study to prove and validate different optimization techniques. The SQP method was applied in [7] to a linear actuator after validation of a shape sensitivity analysis of magnetic forces by the Maxwell Stress Tensor principle and FEM. Improvement of static characteristic of an electromagnet was made in [8] by the same tool.

Based on 3-D FEM and RSM, the SLP method was used in [9] to optimize a permanent magnet linear actuator with moving magnet for driving a needle in a knitting machine.

In [10] is described an optimization strategy of the average value of the electromagnetic force developed by an actuator.

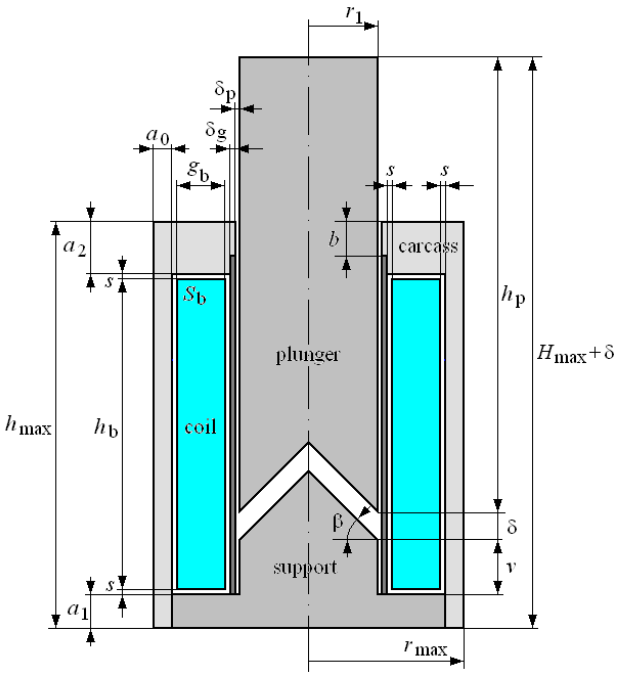

Fig. 1. Geometry of DC electromagnet [14].

The maximization of the clamping force of an electromagnetic linear actuator with divided coil excitation is successfully performed in [11] by using RSM.

The coupling of RSM with 2-D FEM was applied in [12] to develop mathematical relationships between input design parameters and output performance parameters of a tubular permanent magnet brushless linear motor with Halbach magnet array, in order to optimize its efficiency, specific power and cost.

In [13], a method for design optimization of permanent magnetic actuators for medium-voltage-class vacuum circuit breakers is discussed. The RSM and FEM are used to minimize the weight of permanent magnet and to improve the dynamic characteristics.

In recent papers [14], [15] were presented optimal solutions of a DC electromagnet (Fig. 1) providing a maximized static force characteristic [14], respectively, a maximum electromagnetic force related to the largest air-gap (acting force) [15], preserving the global dimensions of the device and the cross-section of the winding. The used tools were DOE and 2-D FEM.

The screening of the DC electromagnet according to three adjustable geometrical parameters has proved that the coil shape ratio k_b, the support thickness ratio k_{a1} and the support height ratio k_v have best influence on the static force characteristic, with more than 80% confidence

$$k_b = \frac{h_b}{g_b} \in [6 \div 8] \quad (1)$$

$$k_{a1} = \frac{a_1}{a} \in [0.9 \div 1.1] \quad (2)$$

$$k_v = \frac{v}{h_b} \in [0.15 \div 0.20] \quad (3)$$

where a = 14.90 mm is the initial value of support thickness.

The first two parameters, exceeding 85% confidence level were taken into account to maximize the static characteristic in [14] and all the three parameters were used to maximize the acting force in [15].

This paper carries out previous analyses proposing an optimal shape of the same DC device, subject to the same constraints, expanding research on a fourth geometrical parameter called support top ratio, k_β, that characterizes the top of the support

$$k_\beta = \frac{\beta}{\beta_1} \in [0.67 \div 1.33] \quad (4)$$

where $\beta_1 = 45°$ is initial value of the angle β.

The design methodology [16] indicates the initial values of geometrical parameters with their ranges and Table I summarizes them [14]. The air-gap varies in range δ = [1 ÷ 41] mm, the winding has N = 1269 turns of standard diameter d = 0.8 mm and the rated voltage is U_r = 110 V DC. For δ = [10 ÷ 41] mm and δ = [1 ÷ 10] mm the currents are I_1 = 12.92 A, respectively, I_2 = 6.90 A, depending on absence or presence of an economy resistor. In Fig. 2 are done the magnetization curves of the core of steel (plunger with support) and of the carcass of cast iron [14].

II. Screening of Device

A screening was performed by numerical experiments with four geometrical parameters: the coil shape ratio k_b, the support thickness ratio k_{a1}, the support height ratio k_v and the support top ratio k_β, looking for their influence on acting force. The used tool to perform the numerical experiments was the FEMM software based on FEM, linked to the LUA language to edit command files. The Maxwell Stress Tensor principle was used to determine the electromagnetic force.

TABLE I.
Geometrical Parameters of DC Electromagnet [14]

r_1 (mm)	29.80	g_b (mm)	19.83	b=0.671a_2 (mm)	10.00
β_1 (°)	45.00	h_b (mm)	138.90	δ_p (mm)	1.00
a_1 (mm)	14.90	s (mm)	2.00	δ_g (mm)	2.00
a_2 (mm)	14.90	v (mm)	24.29	S_b=$g_b h_b$ (mm^2)	2752.27
a_0 (mm)	9.07	h_p (mm)	192.00		

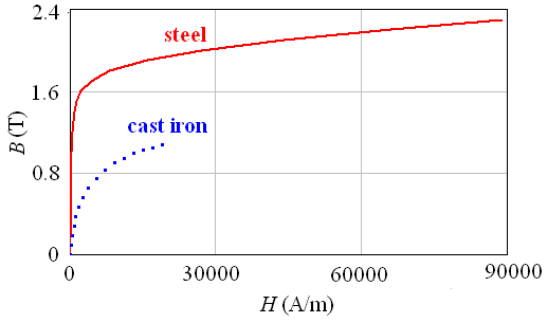

Fig. 2. Magnetization curves for core (plunger with support) (steel) and for carcass (cast iron) [14].

The results of screening are done in Table I that presents the ratio F_{obs} (observed value of a variable F of Fisher-Snedecor type with 1 and 11 degrees of freedom) the effect E and the probability $P(F \le F_{obs})$ for each of the four parameters and of their interactions [4], [14].

For the confidence level of P = 1 - α = 99%, all the analyzed parameters have significant influence on acting force: P_{kb} = 99.999996%, P_{ka1} = 99.608219%, P_{kv} = 99.465511% and $P_{k\beta}$ = 99.999999%, the last being the most influent parameter. Therefore, none of them should be rejected.

The histogram of effects is presented in Fig. 3. The interaction between the first two parameters is stronger than the others ($P_{kb\text{-}ka1}$ = 99.026195%). This study indicates that all the four parameters must be taken into account to maximize the acting force.

TABLE II.
Results of Screening

Source of variation	$F_{obs}(m)$	Effects $E(x_m)$	Probability $P_m = 1 - \alpha_m$
k_b	176.722	-36.700	0.99999996
k_{a1}	13.218	-10.037	0.99608219
k_v	11.963	-9.549	0.99465511
k_β	1089.308	91.116	0.99999999
$k_b \cdot k_{a1}$	9.739	-8.615	0.99026195
$k_b \cdot k_v$	0.008	-0.245	0.06902533
$k_b \cdot k_\beta$	0.040	-0.551	0.15448760
$k_{a1} \cdot k_v$	0.242	-1.358	0.36752407
$k_{a1} \cdot k_\beta$	0.015	0.342	0.09636696
$k_v \cdot k_\beta$	0.752	2.394	0.59563868
$k_b \cdot k_{a1} \cdot k_v$	0.070	0.728	0.20309925
$k_b \cdot k_{a1} \cdot k_\beta$	0.021	-0.404	0.11372498
$k_b \cdot k_v \cdot k_\beta$	0.075	0.758	0.21119270
$k_{a1} \cdot k_v \cdot k_\beta$	0.006	-0.215	0.06072319
$k_b \cdot k_{a1} \cdot k_v \cdot k_\beta$	0.032	0.494	0.13871145
Total	F_{obs}_99% = 9.646, E_99% = 8.574		

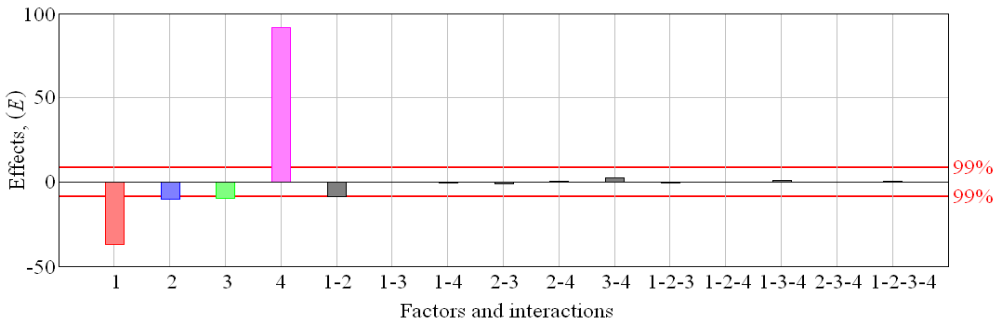

Fig. 3. Histogram of effects.

III. Optimization Problem

The optimization problem is the maximization of the electromagnetic force at δ = 41 mm, calling acting force (F_a), which is set as objective function. This is a 4-D nonlinear optimization problem subject to four equality constraints consisting in preserving the global dimensions of the device (the external radius r_{max}, the height of carcass h_{max}, the height of plunger with support H_{max}) and the coil cross section ($S_b = g_b \cdot h_b$). The complete form (P) of the optimization problem is [12]

$$\mathrm{P}:\begin{cases}\min F_a(k_b,k_{a1},k_v,k_\beta,a_0,a_2,h_p,g_b)\\ k_{b\min}\le k_b\le k_{b\max}\\ k_{a1\min}\le k_{a1}\le k_{a1\max}\\ k_{v\min}\le k_v\le k_{v\max}\\ k_{\beta\min}\le k_\beta\le k_{\beta\max}\\ g_r(k_b,k_{a1},k_v)=0\\ g_h(k_b,k_{a1},k_v)=0\\ g_H(k_b,k_{a1},k_v)=0\\ g_{Sb}(k_b,k_{a1},k_v)=0\end{cases} \quad (5)$$

$$g_r(k_b)=r_1+\delta_p+\delta_g+2s+g_b(k_b)+a_0(k_b)-r_{max} \quad (6)$$

$$g_h(k_b,k_{a1})=k_{a1}a+a_2(k_b,k_{a1})+2s+k_b\cdot g_b(k_b)-h_{max} \quad (7)$$

$$g_H(k_b,k_{a1},k_v)=h_p(k_b,k_{a1},k_v)+k_v\cdot k_b\cdot g_b(k_b)+k_{a1}\cdot a-H_{max} \quad (8)$$

$$g_{Sb}(k_b)=k_b\cdot[g_b(k_b)]^2-S_b \quad (9)$$

where a = 14.90 mm, r_{max} = 65.70 mm, h_{max} = 172.60 mm, H_{max} = 231.19 mm, S_b = 2752.27 mm^2 are initial values resting constant.

Solving the optimization problem is made using the method by zooms without computation of models [4], [12]. This is a method which better fits with DOE. The algorithm iteratively performs a full factorial design. Thus, is analyzed a 4-D rectangular area whose vertices and center correspond to $2^4 + 1 = 17$ numerical experiments.

The point with better response is chosen as center of the next 4-D domain having equal or lower volume compared to the previous.

Different stopping criterions limit the number of iterations, when the accuracy is acceptable [12].Thus, the extreme values per iteration of the response function F_a ($f_{a\,min}$ and $f_{a\,max}$) are compared with the global extreme values ($F_{a\,min}$ and $F_{a\,max}$)

$$\varepsilon\,[\%]=\frac{f_{a\max}-f_{a\min}}{F_{a\max}-F_{a\min}}\cdot 100\le\varepsilon_{max}\,[\%] \quad (10)$$

or the value computed per iteration (t) is compared with the previous different one (s) ($1\le s\le t-1$)

$$\varepsilon_{Fa}\,[\%]=\frac{F_a^{(t)}-F_a^{(s)}}{F_a^{(s)}}\cdot 100\le\varepsilon_{Fa\max}\,[\%] \quad (11)$$

In Fig. 3 are presented the variations of the parameters along the 10-th iterations of the optimization algorithm.

The graphical illustration of the application of the algorithm can be seen in Fig. 4.

The 4-D feasible domain is presented in original way in 3-D view as a surface (in white) on the plane (in gray) described by four positive axes in star disposition, corresponding to the four analyzed parameters.

At each iteration, the calculated values of parameters form the corners of a quadrilateral. The optimal values form the higher quadrilateral corresponding to the maximum acting force.

In Table II are summarized the calculated values. Figure 5 presents the 2-D view.

The 10-th iteration offers the optimal solution k_b = 6.25625, k_{a1} = 0.9046875, k_v = 0.1505859375 and k_β = 1.3313802083 corresponding to the best response F_a = 804.399 N with the errors ε = 1.86%, respectively ε_{Fa} = 0.09%.

The last three optimal computed values of the parameters are closed to the limits of their ranges: k_{a1}, k_v and k_β. The first of them, k_b, stabilizes inside its range.

These can be compared with their initial values k_b = 7, k_{a1} = 1, k_v = 0.175, k_β = 1 and F_a = 663.71 N.

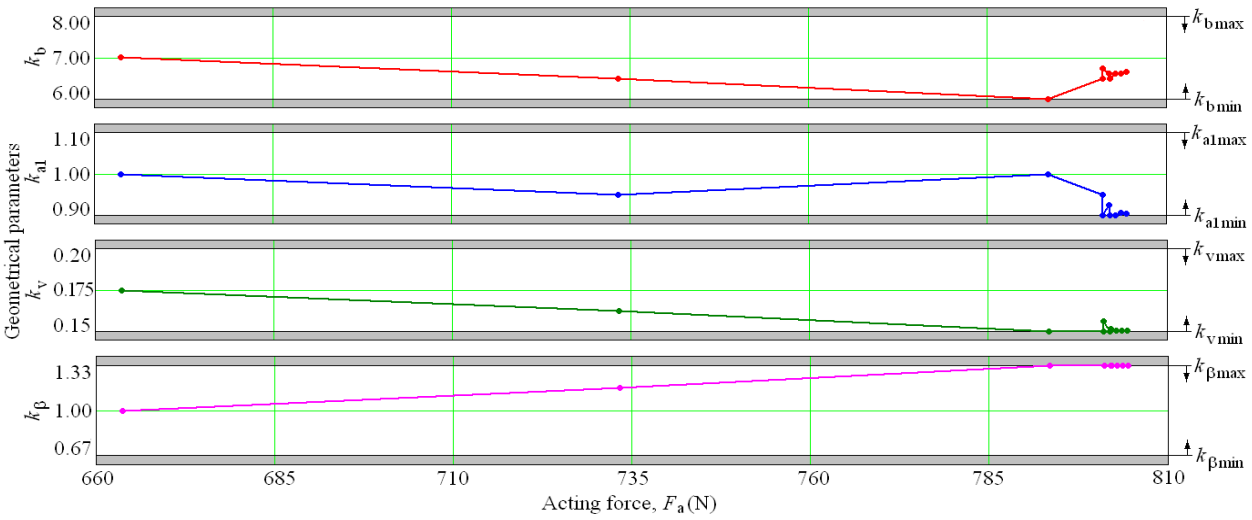

Fig. 3. Variations of the parameters during optimization algorithm.

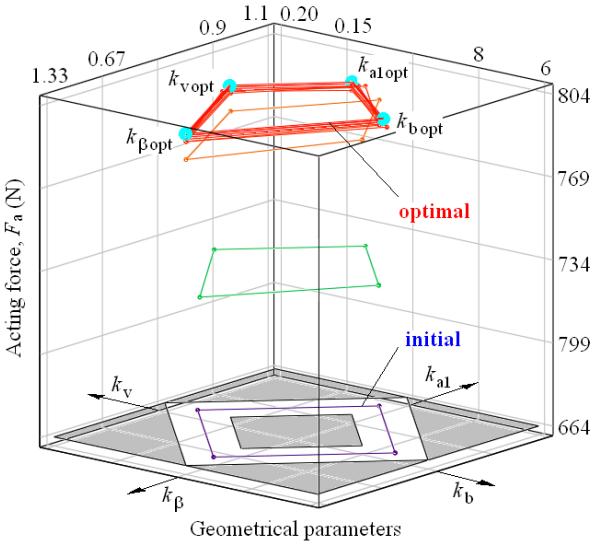

Fig. 4. Four-dimensional feasible domain (white surface on gray plane) and graphical view of iterations of optimization algorithm (3-D view).

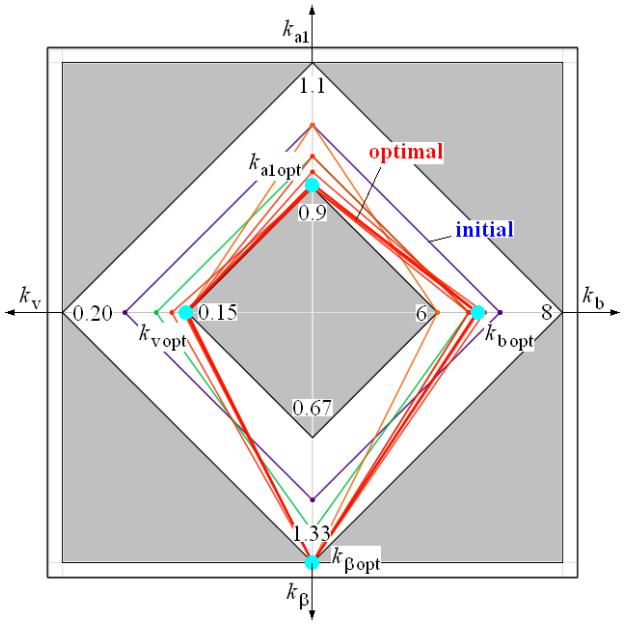

Fig. 5. Four-dimensional feasible domain (white surface on gray plane) and graphical view of iterations of optimization algorithm (2-D view).

TABLE III.
OPTIMIZATION PROCESS: FEM BASED VALUES OF OBJECTIVE FUNCTION F_a AND GEOMETRICAL PARAMETERS

Iter.	N_{tot}	N_{rec}	k_b	k_{a1}	k_v	k_β	F (N)	ε (%)	ε_{Fa} (%)	g_b (mm)	h_b (mm)	a_1 (mm)	a_2 (mm)	a_0 (mm)	v (mm)	h_p (mm)	β (°)
0	-	-	7.00000	1.00000	0.17500	1.00000	663.711	-	-	19.83	138.80	14.90	14.90	9.07	24.29	192.00	45.00
1	17	1	6.50000	0.95000	0.16250	1.16667	733.265	100.00%	10.48%	20.58	133.75	14.15	20.69	8.32	21.73	195.30	52.50
2	17	0	6.00000	1.00000	0.15000	1.33333	793.401	67.58%	8.20%	21.42	128.51	14.90	25.19	7.48	19.28	197.02	60.00
3	17	0	6.50000	0.95000	0.15000	1.33333	801.059	37.97%	0.97%	20.58	133.75	14.15	20.69	8.32	20.06	196.97	60.00
4	17	1	6.50000	0.95000	0.15000	1.33333	801.059	21.35%	0.00%	20.58	133.75	14.15	20.69	8.32	20.06	196.97	60.00
5	17	0	6.62500	0.92500	0.15000	1.33333	802.003	12.81%	0.12%	20.38	135.03	13.78	19.78	8.52	20.25	197.15	60.00
6	17	0	6.50000	0.90000	0.15156	1.33333	802.149	8.76%	0.02%	20.58	133.75	13.41	21.44	8.32	20.27	197.51	60.00
7	17	0	6.62500	0.90000	0.15078	1.33333	802.872	5.72%	0.09%	20.38	135.03	13.41	20.16	8.52	20.36	197.42	60.00
8	17	3	6.62500	0.90625	0.15078	1.33073	803.673	4.29%	0.10%	20.38	135.03	13.50	20.06	8.52	20.36	197.33	59.88
9	17	0	6.62500	0.90625	0.15078	1.33073	803.673	2.88%	0.00%	20.38	135.03	13.50	20.06	8.52	20.36	197.33	59.88
10	17	0	6.65625	0.90469	0.15058	1.33138	804.399	1.86%	0.09%	20.33	135.35	13.48	19.77	8.57	20.38	197.33	59.91
Total	170	5															

The rest of optimal geometrical parameters are done in Table III. The number of the necessary experiments imposed up to the 10-th iterations is N_{tot} = 170, but the number of the points which can be recuperated is N_{rec} = 5, resulting 165 numerical experiments.

In the Fig. 6 can be seen the static force characteristic F for initial and optimal configurations and the opposite force characteristic F_{opp} of springs system.

A significant counterclockwise rotation of initial characteristic is observed. This can perturb the device operation for lower air-gaps when the opposite force becomes important. Therefore, to assure a great enough electromagnetic force to attract the plunger in this range, the economy resistor will be eliminated, keeping the current supply to its initial value, $I'_2 = I_1 = 12.92$ A.

The geometrical shape determined by computed optimal parameters achieved 21.20% improvement in acting electromagnetic force, respectively 140.69 N in addition to 663.71 N, corresponding to the largest air-gap δ = 41 mm.

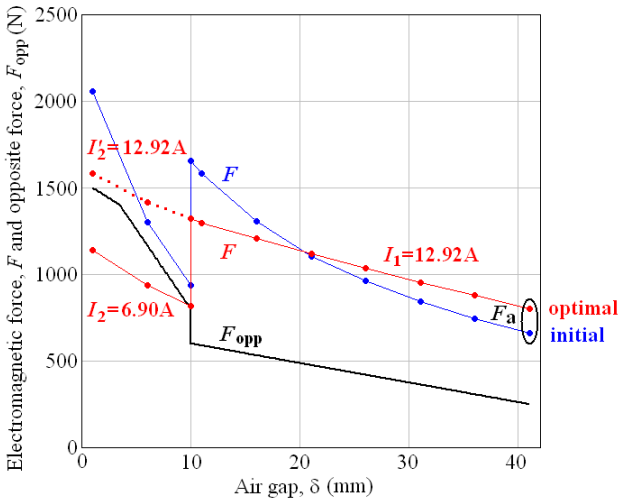

Fig. 6. Static force characteristic F for initial and optimal configurations and opposite force characteristic F_{opp}.

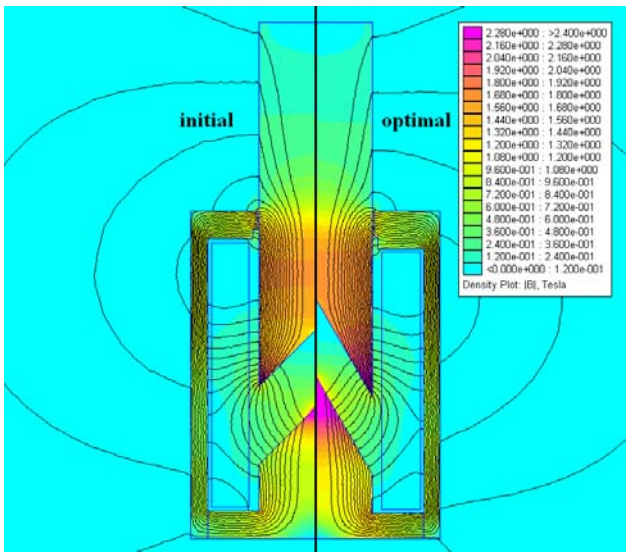

Fig. 7. Distribution of magnetic flux density for initial (left) and optimal (right) shapes (δ = 41 mm, FEMM, axisymmetric solution).

Figure 7 presents on left and right sides the initial and the optimal geometrical shapes with the distributions of magnetic flux density obtained in FEMM software as axisymmetric solution.

IV. Conclusions

An optimal geometrical shape for a DC electromagnet is obtained using DOE and the 2-D FEM.

The optimization problem takes into account four geometrical parameters: the coil shape ratio, the support thickness ratio, the support height ratio and the support top ratio and consists of maximization of acting force related to the largest air-gap, preserving the global dimensions of DC electromagnet and the cross-section of the winding.

A previous screening of the device proves with 99% confidence the best influence of the above parameters on the acting force.

Using the optimization method by zooms without computation of models, the acting force is increased by 21.20% with the cost of reduction of electromagnetic force for lower air-gaps which can be compensated by eliminating the economy resistor in this range.

Acknowledgment

Source of research funding in this article: Research program of the Electrical Engineering Department financed by the University of Craiova.

Contribution of authors:

First author – 100%

Received on July 29, 2017

Editorial Approval on October 15, 2017

References

[1] D. Montgomery, Design and analysis of experiment, 5-th Edition, Arizona State University, 2000.

[2] F. Gillon, "Modelisation et optimisation par plans d'experiences d'un moteur a commutations electronique," Ph-D Thesis, Lille, 1997.

[3] M. Caldora-Costa, "Optimisation de dispositifs electromagnetiques dans un contexte d'analyse par la methode des elements finis," Ph-D Thesis, Grenoble, 2001.

[4] S. Vivier, "Strategies d'optimisation par la methode des plans d'experiences et applications aux dispositives electrotechniques modelise par elements finis," Ph-D Thesis, Lille, 2002.

[5] F. Gillon, and P. Brochet, "Screening and response surface method applied to the numerical optimization of electromagnetic devices," IEEE Transaction on Magnetics, Vol. 36, No. 4, pp.1163-1166, 2000.

[6] D.-K. Hong, K.-C. Lee, B.-C. Woo, and D.-H. Koo, "Optimum design of electromagnet in magnetic levitation system for contactless delivery application using response surface methodology," Proceedings of the 2008 International Conference on Electrical Machines, pp. 1-6, 2008.

[7] J.-M. Biedinger, and D. Lemoine, "Shape sensitivity analysis of magnetic forces", IEEE Trans.on Magn.,Vol.30, pp. 2309-2516, 1997.

[8] G. Sefkat, "The design optimization of the electromechanical actuator," Structural and Multidisciplinary Optimization, February 2009, Volume 37, Issue 6, pp. 635–644, 2009.

[9] I. Yatchev, M. Rudnicki, K. Hinov, and V. Gueorgiev, "Optimization of a permanent magnet needle actuator," COMPEL, Vol. 31, Issue 3, pp. 1018-1028, 2012.

[10] S. Yong, J. Tong, S. Enze, and Y. Zaiming, "Analysis and optimization of static characteristics in overall operating conditions of electromagnetic actuator," Research Journal of Applied Sciences, Engineering and Technology 7(8), pp. 1561-1567, 2014.

[11] T.-W. Kim, and J.-H. Chang, "Optimal design of electromagnetic actuator with divided coil excitation to increase clamping force," Journal of International Conference on Electrical Machines and Systems, pp. 1461-1464, 2014.

[12] K. Li, X. Zhang, and H. Chen, "Design Optimization of a Tubular Permanent Magnet Machine for Cryocoolers", IEEE Transactions on Magnetics, Vol. 51, pp.1-8, 2015.

[13] H.-M. Ahn, T.-K. Chung, Y.-H. Oh, K.-D. Song, Y.-I. Kim, H.-R. Kho, M.-S. Choi, and S.-C. Hahn, "Optimal Design of Permanent Magnetic Actuator for Permanent Magnet Reduction and Dynamic Characteristic Improvement using Response Surface Methodology," J. Electr. Eng. Technol.2015, 10(3): pp. 935-943, 2015.

[14] A.-I. Dolan, "Optimization of DC electromagnet using design of experiments and FEM," XIII-th IEEE International Conference on Applied and Theoretical Electricity – ICATE 2016, Craiova, Romania, October 06-08, pp. 1-6, 2016.

[15] A.-I. Dolan, "Three parameters optimization of acting force of DC electromagnet," Proceedings of 11-th IEEE International Conference on Electromechanical and Power Systems – SIELMEN 2017, Iasi-Chisinau, October 11-13, pp. 1-4, 2017.

[16] G. Hortopan, Electrical apparatus of low voltage (in Romanian), Tehnica Publishing House, Bucharest, 1969.